Journal of Radiation Research, 2013, 54, 182–189
doi: 10.1093/jrr/rrs068 Advance Access Publication 21 August 2012

Dosimetric differences among volumetric modulated arc radiotherapy (RapidArc) plans based on different target volumes in radiotherapy of hepatocellular carcinoma

GuanZhong GONG, Yong YIN*, YuJie GUO, TongHai LIU, JinHu CHEN, Jie LU, ChangSheng MA, Tao SUN, Tong BAI, GuiFang ZHANG, DengWang LI and RuoZheng WANG

Department of Radiation Oncology, Shandong Cancer Hospital, 440 Jiyan Road, Jinan, 250117, China
*Corresponding author. Department of Radiation Oncology, Shandong Cancer Hospital, Shandong Provincial Key Laboratory of Radiation Oncology, Shandong Academy of Medical Sciences, 440 Jiyan Road, 250117 Jinan, China. Tel: +86-531-6762-6524; Fax: +86-531-6762-6427; Email: yinyongsd@yahoo.com.cn

(Received 6 February 2012; revised 10 July 2012; accepted 11 July 2012)

We investigated the dosimetric differences among volumetric-modulated arc radiotherapy (RapidArc, RA) plans designed for various target volumes in hepatocellular carcinoma (HCC). Ten HCC patients underwent 3D-CT scanning at free breathing (FB), 3D-CT at end inspiration hold (EIH) assisted by an Active Breathing Coordinator (ABC), and 4D-CT scanning. Gross tumor volumes (GTVs) were manually contoured on CT images. The individualized internal gross target volume ($IGTV_1$) was obtained from 10 GTVs from 4D-CT images. Tumor individual margins were measured from GTV_{FB} to $IGTV_1$. The $IGTV_2$ was obtained from GTV_{FB} by applying individual margins. Four planning target volumes ($PTV_{1\text{-}4}$) were obtained from $IGTV_1$, $IGTV_2$, GTV_{FB}, and GTV_{EIH}, respectively. An RA plan was designed for each of the PTVs ($RA_{1–4}$). One 358° arc was used for $PTVs_{1–3,}$ while three 135° arcs were used for PTV_4. It was found that PTV_2 and PTV_3 were larger than PTV_1 and PTV_4. The mean values of PTV_3/PTV_1 and PTV_3/PTV_4 were 2.5 and 1.9, respectively. The individual margins in the X, Y and Z axial directions varied greatly among these patients. There were no significant differences in the conformal index or homogeneity index among the four RA plans. RA_1 and RA_4 significantly reduced the radiation dose of normal liver tissue compared with RA_2 and RA_3 ($P < 0.01$). There were no significant differences between the radiation doses of the stomach and duodenum. RapidArc combined with 4D-CT or ABC technology is a promising method in radiotherapy of HCC, and accurately targeted the tumor volume while sparing more normal liver tissue.

Keywords: hepatocellular carcinoma; radiotherapy; intensity-modulated arc radiotherapy; dosimetry

INTRODUCTION

Hepatocellular carcinoma (HCC) is one of the most prevalent tumors worldwide, often developing secondary to either a hepatitide infection (hepatitis B or C) or liver cirrhosis [1, 2]. Current treatment options include surgery, transarterial chemoembolization (TACE) [3], radiotherapy (RT), and molecular target therapy [4, 5]. RT has become an especially important treatment option for patients with unresectable HCC [6]. Whole liver RT is rarely performed, to avoid irradiation dose of normal liver tissue [7]. In recent years RT technologies have been developed that enable localized radiation delivery, and three dimensional conformal RT (3D-CRT) and intensity-modulated RT (IMRT) have been used to treat HCC. These techniques are highly efficient, and spare more normal liver tissue. It has also been shown that RT combined with TACE can improve the survival of HCC patients [8]. However, radiation-induced liver disease, the most severe complication of RT with a mortality rate of 76%, cannot be overlooked. Prevention is the best way to avoid radiation-induced liver disease [9].

Because respiratory movement easily influences the position of the liver tumor, accurately locating the target volume for HCC RT is extremely important. The traditional method of ensuring adequate target volume coverage is to expand margins (sometimes perhaps excessively) to what is

known as the gross tumor volume (GTV) [10]. However, it is impossible to obtain absolutely safe margins because of differences in patients' respiratory movements and the effect of these movements on tumor position, shape and volume [11].

In recent years, Active Breathing Coordinator (also known as active breath control, or ABC) and four dimensional (4D)-computed tomography (CT) techniques have been used in clinical RT practice for HCC and other cancers, and have shown promising results [12–15]. In addition, an improved form of IMRT, which replaces fixed-field radiation methods, is volumetric-modulated arc therapy (VMAT). VMAT rotates the radiation beam around the patient so that the tumor is treated from all angles. A commercially available variation of VMAT is RapidArc™ (Varian Medical Systems, Palo Alto, CA). RapidArc is image-guided, and delivers the radiation dose with a single continuous 360° motion in < 2 min. Parameters include the gantry's rotation speed, the size and shape of the beam controlled by a dynamic multi-leaf collimator, and the rate of dose delivery. RapidArc and Elekta VMAT (Pinnacle 9 SmartArc, Philips) can achieve better dose distributions than conventional IMRT with much shorter treatment times and a reduction in monitor units (MU; a measure of scatter radiation) [16, 17].

RapidArc requires accurate delineation of the target volume to achieve perfect dose delivery. Geometric inaccuracy will drastically affect the target volume coverage. Most research on RapidArc has been based on one or two whole arcs of 358°, or >180°. However, due to treatment time and mechanical limitations, RapidArc treatment plans that include gating or ABC have not been reported in the literature [17]. In this study, we investigated the dosimetric features of RapidArc plans for HCC RT, by applying different target volumes.

MATERIALS AND METHODS

Patients

Ten patients with pathologically proven HCC were included. These patients were randomly selected from a list of patients who were treated in our hospital between March 2010 and January 2011. There were two women and eight men with an average age of 56 years (age range: 52–60 years). Cardiopulmonary function was tested before this study and the breathing hold time of each patient was >30 s [18]. All patients had good cardiopulmonary function, communicated well with the medical staff, and could coordinate their breathing with the ABC. All the patients accepted TACE treatment in our hospital.

The Research Ethics Board of Shandong Cancer Hospital approved this clinical trial. Each patient provided informed written consent.

CT simulation and plannning target volume (PTV) acquisition

The simulations were performed with a Brilliance Big Bore CT scanner (Phillips Medical Systems, Highland Heights, OH) connected to an Elekta Active Breathing Coordinator™ system (Elekta Synergy, Crawley, UK) and a Varian Real-Time Position Management system (Varian Medical Systems, Palo Alto, CA).

Prior to simulation, patients were given breathing training. The breath trigger threshold values and the longest end inspiration hold (EIH) times were recorded. The patients were immobilized with a vacuum pillow with their arms raised above their heads. The CT scan region extended from 4 cm above the upper edge of the diaphragm to 4 cm below the lower edge of the right kidney. The 4D-CT scans were performed and progress was monitored by the ABC. After the 4D-CT scan, 3D-CT scans were subsequently performed in free breathing (CT_{FB}) and end inspiration hold (CT_{EIH}) assisted by the ABC. The 4D-CT images were sorted into 10 CT series according to the respiratory cycle, labeled CT_0, $CT_{10} \ldots CT_{90}$ (i.e. CT_0 for the end inspiration phase, CT_{20} for the respiratory intermediate phase, and CT_{50} for the end expiratory phase) [19]. The CT images were transmitted to the Eclipse system (V8.6.15, Varian Medical Systems, Palo Alto, CA) for target volume contouring and treatment planning.

Corresponding GTVs were delineated by using the same window width (200 HU) and window level (40 HU) on CT_0, $CT_{10} \ldots CT_{90}$, CT_{FB} and CT_{EIH}, and labeled GTV_0, $GTV_{10} \ldots GTV_{90}$, GTV_{FB} and GTV_{EIH}, respectively. To reduce potential errors in contouring, all GTVs were determined by two doctors from the Department of Radiation Oncology from contrasted diagnostic CT or MRI images. The GTVs of one patient are shown in Figs 1 and 2.

GTV_0, $GTV_{10} \ldots GTV_{90}$ were merged into an internal gross target volume ($IGTV_1$), and then the margins from GTV_{FB} to $IGTV_1$ in the X, Y and Z axial coordinate directions were obtained. $IGTV_2$s were obtained from GTV_{FB} using these margins, as shown in Fig. 2. PTVs were obtained based on $IGTV_1$, $IGTV_2$, GTV_{FB}, and GTV_{EIH} [20]. PTV_1 and PTV_2 were obtained from $IGTV_1$ and $IGTV_2$, plus 5-mm margins isotropically [14]. PTV_3 was obtained from GTV_{FB} using 2-cm margins in the craniocaudal direction, and 1.5-cm margins in the medial-lateral and anteroposterior directions [8, 19]. PTV_4 was obtained from GTV_{EIH} using 8-mm margins isotropically [12] (Fig. 3). The flow chart of our study is shown in Fig. 4. Organs at risk (OARs), which included the liver, stomach, and duodenum, were also delineated. The normal liver was defined as the liver volume minus the PTV, and labeled as normal $liver_1$, normal $liver_2$, normal $liver_3$ and normal $liver_4$ (Figs 1–4).

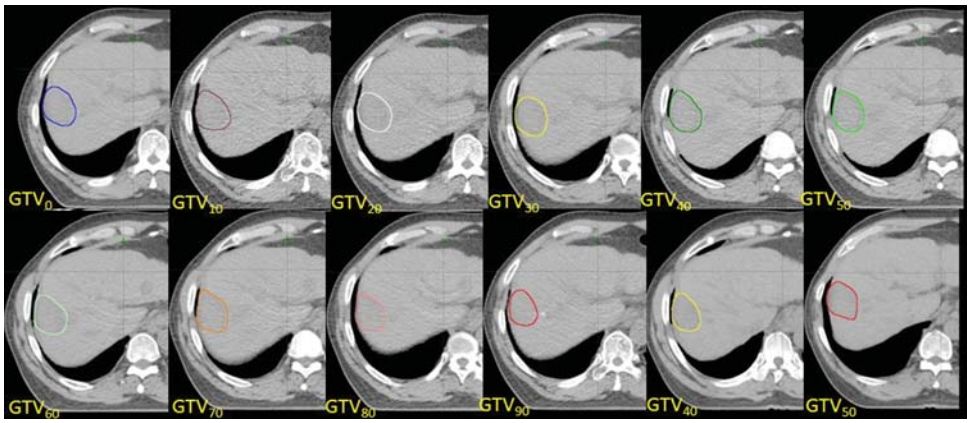

Fig. 1. The GTVs of one patient, (GTV_0: 11.34 cm^3, GTV_{10}: 11.39 cm^3, GTV_{20}: 11.67 cm^3, GTV_{30}: 11.66 cm^3, GTV_{40}: 11.98 cm^3, GTV_{50}: 11.99 cm^3, GTV_{60}: 11.57 cm^3, GTV_{70}: 11.49 cm^3, GTV_{80}: 11.47 cm^3, GTV_{90}: 11.9 cm^3, GTV_{FB}: 18.04 cm^3, GTV_{EIH}: 11.06 cm^3).

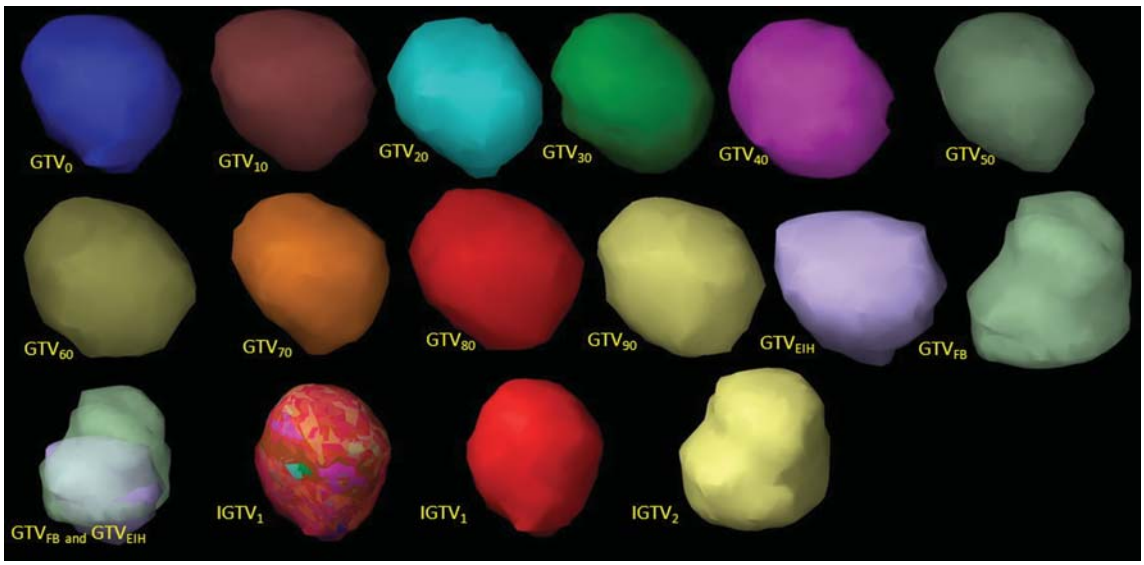

Fig. 2. The shape of GTVs and IGTVs. Because of repeat scanning in 3D-CT_{FB}, the GTV_{FB} was larger than other GTVs, and $IGTV_2$ was larger than $IGTV_1$ ($IGTV_1$: 20.09 cm^3, $IGTV_2$: 42.49 cm^3).

Design of the RT plans

RapidArc plans were individually designed for the different PTVs. For PTV_1, PTV_2, and PTV_3, one single 358° arc was applied. For PTV_4, three 135° arcs were used, the three fields were optimized simultaneously, and two arcs were allowed to overlap in the liver region. The plans were labeled RapidArc $(RA)_1$, RA_2, RA_3, and RA_4, respectively. A dose of 50 Gy was prescribed in 25 fractions (2.0 Gy/fraction) at the isocenter with an inhomogeneity correction. The tumor dose coverage requirements were that the PTV should be covered by a 95% isodose volume and inhomogeneity < 10%. The dose constraints for OARs were: mean dose of normal liver ≤23 Gy, and the dose-volume histogram of the normal liver within the tolerance area (i.e. a V_5 of <86%, $V_{10} < 68\%$, $V_{15} < 59\%$, $V_{20} < 49\%$, $V_{25} < 35\%$, $V_{30} < 28\%$, $V_{35} < 25\%$ and $V_{40} < 20\%$) [21]. For the stomach and duodenum, the maximum dose was limited to 45 Gy and the volume receiving >25 Gy was limited to <5 cm^3 [22].

The optimization objectives for all plans were set as: 98% of the volume of the PTV to reach 95% of the prescription dose with 10% of the volume of PTV, not exceeding 110% of the prescription dose. The 100% prescription dose of all plans was set to normalize the PTV mean dose.

All plans were designed and optimized for Varian Trilogy, equipped with a multi-leaf collimator with a leaf

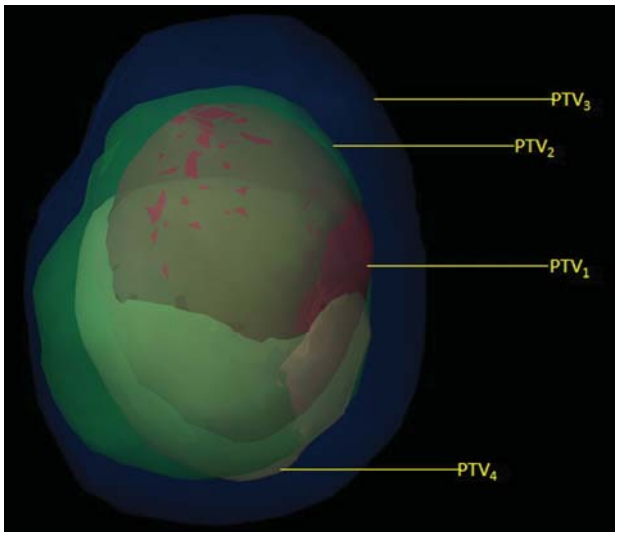

Fig. 3. The different PTVs. $PTV_{1\ (red)}$: 46.16 cm^3, $PTV_{2\ (green)}$: 83.98 cm^3, $PTV_{3\ (blue)}$: 167.83 cm^3, and $PTV_{4\ (yellow)}$: 48.19 cm^3.

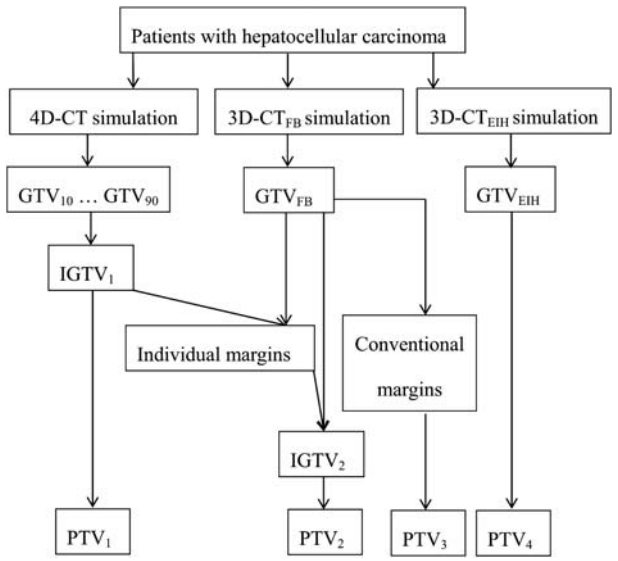

Fig. 4. Flow chart for obtaining the GTVs, IGTVs, and PTVs.

width of 5 mm at the isocenter. All dose distributions were computed with the Analytical Anisotropic Algorithm implemented in the Eclipse v8.6 treatment planning system with a calculation grid resolution at 2.5 mm, maximum. The maximum dose rate was set at 600 MU/min.

The dose rate of the RA plan mentioned above was set at maximum during RT. During the actual treatment the dose rate changed whenever necessary to keep the circular motion of the gantry, the shape of the multi-leaf collimator, and the dose delivery uniform; otherwise it could affect the efficiency and the precision of the treatment.

Planning evaluation

For PTV, the $D_{1\%}$ and $D_{99\%}$ (doses to 1% and 99% of the PTV, respectively) were defined as the maximum and minimum doses. The conformal index (CI) was calculated using Van't Riet's definition: $CI = \frac{TV_{RI}}{TV} \times \frac{TV_{RI}}{V_{RI}}$, where TV_{RI} was the target volume covered by the reference isodose, TV was the target volume, and V_{RI} was the volume of the reference isodose. CI ranges from 0 to the ideal value 1. The homogeneity index (*HI*) was defined as: $HI = 1 - \frac{D_{2\%;} - D_{98\%;}}{\text{prescription dose}}$; HR ranges from 0 to the ideal value 1 [21].

The mean radiation dose delivered to the normal liver (D_{mean}), V_5, V_{10}, V_{20}, V_{30} and V_{40} (where V_x represented the percentage of the volume of x Gy in the normal liver), the maximum doses (D_{max}) delivered to the stomach and duodenum, and the radiation dose received by 5 cm^3 of volume were also recorded and compared [23].

Statistical analyses

Statistical analyses were performed using SPSS 16.0 (IBM, Chicago, IL) software. The Friedman test was used to compare three groups of data. Pairwise data were compared using the paired Wilcoxon test. A P-value <0.05 was considered statistically significant.

RESULTS

Volume of liver and normal liver

Ten patients successfully completed the 3D-CT and 4D-CT scans and all the breath holding times were ≤30 s. No complaints of discomfort were reported during the breath training and CT simulations. The maximal liver volume of 10 patients in EIH was 1979.84 cm^3 and the minimal liver volume was 1068.72 cm^3 (average volume: 1533.9870 cm^3). There were no statistical differences among the normal $liver_1$, normal $liver_2$, normal $liver_3$, and normal $liver_4$ ($\chi^2 = 5.040$, $P = 0.169$).

The margins from GTV_{FB} to $IGTV_1$

The margin from GTV_{FB} to $IGTV_1$ varied widely in the same axial direction among patients (Table 1). The margins in the Z axial were larger than the X and Y. The margins in the positive and negative directions on the same axial were equal only in a few patients. The margin difference between the positive and negative directions on the same axial was not statically significant ($P > 0.05$).

Table 1. The margins from GTV_{FB} to $IGTV_1$ in the +X, –X, +Y, –Y, +Z and –Z axial directions

No.	+X	–X	+Y	–Y	+Z	–Z
1	0.70	0.00	0.70	0.00	0.00	0.30
2	0.50	0.30	0.20	0.70	2.00	0.00
3	0.00	0.40	0.50	0.00	0.50	0.50
4	0.50	0.40	0.50	0.30	0.00	0.00
5	1.00	0.60	2.00	0.50	0.20	2.20
6	0.70	0.30	0.20	0.40	2.00	0.80
7	0.30	0.30	0.80	0.50	1.30	1.50
8	0.30	0.30	0.50	0.00	0.00	1.80
9	0.40	0.80	0.60	0.30	1.30	0.80
10	0.30	0.30	0.60	0.60	1.30	0.40
$\bar{x} \pm SD$	0.47 ± 0.28	0.37 ± 0.21	0.66 ± 0.51	0.33 ± 0.26	0.86 ± 0.81	0.83 ± 0.76

Table 2. Comparison of different indices among RA_1, RA_2, RA_3 and RA_4

	RA_1	RA_2	RA_3	RA_4	χ^2	P
PTV (cm^3)	56.64 ± 38.54	82.00 ± 46.73	131.75 ± 76.63	68.74 ± 45.63	22.20	0.00
CI	0.93 ± 0.05	0.94 ± 0.02	0.94 ± 0.02	0.93 ± 0.03	3.72	0.293
HI	0.91 ± 0.01	0.91 ± 0.01	0.90 ± 0.02	0.91 ± 0.01	7.56	0.056
$D_{1\%}$ (Gy)	54.44 ± 0.36	54.43 ± 0.51	54.94 ± 0.82	54.68 ± 0.47	5.60	0.086
$D_{99\%}$ (Gy)	49.18 ± 0.48	49.27 ± 0.70	48.67 ± 0.57	49.00 ± 0.34	5.88	0.118
D_{mean} (Gy)	8.23 ± 1.5	9.62 ± 3.4	10.21 ± 4.5	7.63 ± 3.00	10.68	0.014
V_5 (%)	46.64 ± 19.31	51.00 ± 22.50	54.49 ± 24.90	43.29 ± 19.94	9.48	0.024
V_{10} (%)	28.73 ± 11.54	36.12 ± 16.29	38.86 ± 19.53	28.23 ± 12.37	10.44	0.015
V_{15} (%)	17.87 ± 6.61	22.55 ± 10.53	26.54 ± 14.22	18.20 ± 7.55	11.88	0.008
V_{20} (%)	11.62 ± 4.39	14.58 ± 6.77	17.76 ± 9.12	11.83 ± 4.58	13.68	0.003
V_{25} (%)	7.71 ± 2.91	9.34 ± 4.11	11.78 ± 5.55	7.58 ± 2.79	14.04	0.003
V_{30} (%)	5.14 ± 2.01	6.12 ± 2.54	7.76 ± 3.36	5.05 ± 1.79	14.76	0.002
V_{35} (%)	3.41 ± 1.35	3.73 ± 1.35	5.06 ± 2.06	3.35 ± 1.21	13.80	0.003
V_{40} (%)	2.12 ± 0.86	2.47 ± 1.00	3.11 ± 1.21	2.06 ± 0.75	14.88	0.002
Stomach D_{max} (Gy)	13.40 ± 7.10	19.89 ± 12.24	22.64 ± 15.64	12.27 ± 10.96	7.20	0.066
Stomach $D^3_{5\,cm}$ (Gy)	9.53 ± 4.43	12.15 ± 6.84	16.16 ± 12.08	9.43 ± 7.04	7.08	0.069
Duodenum D_{max} (Gy)	19.03 ± 18.90	25.06 ± 18.44	28.06 ± 22.70	21.19 ± 18.44	6.60	0.086
Duodenum $D^3_{5\,cm}$ (Gy)	9.96 ± 10.99	13.12 ± 14.91	12.97 ± 10.98	7.21 ± 9.01	4.44	0.218

The volume of GTVs and PTVs

The mean volumes of GTV_0, GTV_{FB}, and GTV_{EIH} were 14.53, 14.24, and 14.83 cm^3, respectively. There was no statistical difference among the three GTVs ($\chi^2 = 1.077$, $P = 0.584$). The volume of PTV_3 was the largest of the four PTVs. The mean values of PTV_3/PTV_1, PTV_3/PTV_2 and PTV_3/PTV_4 were 2.5, 1.7 and 1.9, respectively. PTV_2/PTV_1 and PTV_4/PTV_1 were 1.60 and 1.27, respectively. The differences among the four PTVs were statistically significant ($P < 0.05$; Tables 2 and 3).

Table 3. The paired comparison results of PTV, D_{mean}, and V_5–V_{40} among RA_1, RA_2, RA_3 and RA_4

	RA_1 vs RA_2		RA_1 vs RA_3		RA_1 vs RA_4		RA_2 vs RA_3		RA_2 vs RA_4		RA_3 vs RA_4	
	Z	*P*	*Z*	*P*	*Z*	*P*	*Z*	*P*	*Z*	*P*	*Z*	*P*
PTV	–2.70	0.007	–2.80	0.005	–2.29	0.022	–2.60	0.009	–1.886	0.059	–2.70	0.007
D_{mean}	–1.58	0.114	–1.68	0.093	–0.89	0.386	–1.38	0.169	–2.00	0.047	–2.50	0.013
V_5	–1.38	0.169	–1.68	0.093	–1.78	0.074	–0.89	0.386	–2.29	0.022	–2.40	0.017
V_{10}	–2.29	0.022	–2.09	0.037	–0.51	0.959	–1.07	0.285	–1.89	0.059	–2.19	0.028
V_{15}	–2.00	0.047	–2.29	0.022	–0.255	0.779	–1.48	0.139	–1.48	0.139	–2.29	0.022
V_{20}	–2.09	0.037	–2.50	0.013	–0.153	0.878	–2.00	0.047	–2.19	0.028	–2.40	0.017
V_{25}	–2.00	0.047	–2.50	0.013	–0.26	0.799	–2.19	0.028	–2.19	0.028	–2.70	0.007
V_{30}	–2.40	0.017	–2.60	0.009	–0.153	0.878	–2.19	0.028	–2.19	0.028	–2.60	0.009
V_{35}	–1.48	0.139	–2.60	0.009	–0.153	0.878	–2.40	0.017	–0.97	0.333	–2.60	0.009
V_{40}	–2.19	0.028	–2.60	0.009	–0.76	0.445	–2.19	0.028	–2.09	0.037	–2.60	0.009

The conformal and homogeneity indices

The mean values of CI and HI in the four RA plans were all larger than 0.90. The differences of CI, HI, $D_{1\%}$ and $D_{99\%}$ among the RA plans were not statistically significant ($P > 0.05$; Table 2).

The radiation dose of OARs

The normal liver D_{mean} value and $V_{5–40}$ in RA_2 and RA_3 were larger than RA_1 and RA_4. The D_{mean} of normal liver was significantly reduced, from 10.21 Gy (RA_3) and 9.62 Gy (RA_2) to 8.23 Gy (RA_1) and 7.63 Gy (RA_4; $P < 0.05$). The mean value of V_{30} decreased from 7.76% (RA_3) and 6.12% (RA_2) to 5.14% (RA_1) and 5.05% (RA_4). There were no significant differences for V_5–V_{40} between RA_1 and RA_4 ($P > 0.05$). The evaluation indices of the stomach and duodenum did not differ significantly ($P > 0.05$; Tables 2 and 3).

DISCUSSION

In recent years RapidArc has been used in clinical practice to treat various tumors [15, 24–27]. Previous research showed that RapidArc could achieve better target coverage than traditional IMRT plans, with a much shorter treatment time and fewer monitor units. Yin and colleagues [27] observed that RapidArc achieved a better CI in HCC RT. With high-dose conformal RT, geometric uncertainty will obviously affect the accuracy of dose delivery. Therefore, accurate determination of the target volume is extremely important when applying RapidArc.

Currently, there are three CT simulation techniques for HCC RT: 3D-CT in free breathing, 3D-CT assisted by ABC, and 4D-CT. 3D-CT in free breathing cannot truly identify tumor location or represent morphology because of movement of the liver during the scanning process; it is necessary to set large margins to ensure adequate coverage, which might increase the normal liver volume within the PTV, and therefore the incidence of radiation-induced liver disease. It is impossible to obtain safe margins due to individual variations in breath movement.

3D-CT assisted by ABC can immobilize the tumor at a specific breathing phase and thus its location is more accurately located. This could be a promising approach to determining the individual target volume.

4D-CT scanning synchronizes CT image acquisition with the respiratory cycle, thereby enabling better analysis of the variables during respiration. Due to its ability to accurately monitor tumor motion, 4D-CT has increasingly been used to predict tumor movement during treatment. Compared with 3D-CT in FB, 4D-CT allows more accurate determination of the IGTV of HCC. The respiration should be steady during 4D-CT scanning; otherwise a portion of the target volume may be cropped-off. In our present study, we investigated the dosimetric differences among RapidArc plans for HCC RT based on different target volumes. Furthermore, we investigated the principles for determining individual margins via 4D-CT.

At the beginning of our study we considered using 3D-CRT and IMRT, but the limited CI of 3D-CRT could not reflect the dosimetric differences among target volumes. The long dose delivery time for every field and fraction was the major limitation of combining IMRT with ABC. RapidArc, which can achieve excellence dose delivery within a shorter treatment time, was the ideal tool to carry out this study.

To accommodate differences in breath status, we used a 358° arc for PTV_1, PTV_2 and PTV_3. For PTV_4, three 135°

arcs were used. The Varian Trilogy was employed as a linear accelerator in our hospital and the angular velocity was set to 4.8°/s. The average treatment time for each field was 28.20 s; there was a 30-s interval for patient rest and gantry preparation twice. Therefore, the treatment can be theoretically completed within 115 s. The size of each arc was limited by the breath holding time of the patient. There is no organ movement during the scan if the time of the scan is limited to within 30 s. The same result was observed in our clinical practice by applying ABC. In order to maintain reproducibility in RT, we do not recommend that the patients hold their breath for a long time. Our research shows that the RA plans using three 135° arcs achieved a similar dose delivery as a single 358° arc.

An adequate and accurate individualized target volume should reduce target volume and spare more healthy tissue. We found in this study that the margins of a few patients are equal in the positive and negative directions of every axial coordinate, and the margins of the same axial could vary greatly among patients. Furthermore, the application of isotropical margins on the same axial might exclude part of the target volume, or conversely include normal tissue that is then irradiated. Thus, it is very important to accurately determine an individualized target volume for HCC. This is consistent with the findings of Hughes *et al*. [28] for RT of non-small cell lung cancer. We also observed that although RA_2 could spare more liver tissue compared to RA_3, individualized margins could not be easily obtained due to the randomness of the target volume position in $3D\text{-}CT_{FB}$. Combining $3D\text{-}CT_{FB}$ and a traditional RT simulator or ultrasound may become an effective way to individualize target volume for HCC in institutions not equipped with ABC or 4D-CT.

The dose delivered to the stomach and duodenum did not differ significantly in our study. Park and colleagues [29] showed an association between dose and tumor response in local RT for primary HCC. They found that the tumor response improved with increased radiation dose, but complications arising from increased RT doses were also observed. Radiation dose to the normal liver was a limiting factor in dose escalation; hepatic toxicity is a major obstacle in radiotherapy for HCC [30].

The results of our study suggest that 4D-CT with ABC can reduce the radiation dose in RT of HCC. This is especially true for the V_{30} and D_{mean} of normal liver. This could lower the incidence of radiation-induced liver disease [31]. It is impossible to obtain individualized margins based on GTV_{FB}, due to the randomness of the liver position. Application of 4D-CT or ABC technology can effectively reduce the radiation dose of normal liver in HCC RT. In the present study, we learned that PTV_1 and PTV_4 could reduce the volume of PTV_3 by 48% and 55%, respectively, on average. It is very important to protect the normal liver tissue and elevate the radiation dose delivered to the PTV when the GTV is very large, and applying 4D-CT or an ABC device can reduce the absolute volume significantly. Therefore, 4D-CT and ABC technology are considered effective methods of protecting normal liver tissue [32]. Although we found that PTV_4 was significantly larger than PTV_3, there was no significant difference in sparing normal liver tissue.

Based on our data, we could not prove whether 4D-CT or ABC is more desirable. Heart and lung function, the patient's coordination and aural comprehension should be considered in selecting 4D-CT or ABC. For young patients with good heart and lung function, the ABC is the preferred treatment option. However, 4D-CT should be considered for patients with incompetent heart and lung function, or poor coordination or aural comprehension.

In the present study, we found that breath training was important in HCC RT. Our previous research proved that 3D-CT and 4D-CT were equal in determining the IGTV [33]. The number of fractions for HCC RT was 15–30, and variations in respiratory motion could easily affect the accuracy of RT. However, this effect could be minimized by setting the appropriate threshold value of ABC. Still, some patients cannot hold their breath as required during RT. Breath training is also essential when applying 4D-CT to determine the target volume.

CONCLUSION

Compared with conventional 3D-CT in FB, VMAT (RapidArc) with 4D-CT or 3D-CT associated with ABC can ensure accuracy in delivery of the target volume during RT for HCC, sparing more normal liver tissue. Applying 4D-CT and ABC were similar in sparing normal liver tissue. VMAT (RapidArc) associated with 4D-CT or ABC is an effective and accurate approach for perfect dose delivery, and will become the principle modality for local precise RT of HCC.

FUNDING

This research was supported by the National Science Foundation of (NIH) of China (NO.81172132).

REFERENCES

1. Rodríguez-Díaz JL, Rosas-Camargo V, Vega-Vega O *et al*. Clinical and pathological factors associated with the development of hepatocellular carcinoma in patients with hepatitis virus-related cirrhosis: a long-term follow-up study. *Clin Oncol (R Coll Radiol)* 2007;**19**:197–203.
2. Fukuhara T, Sharp GB, Mizuno T *et al*. Liver cancer in atomic-bomb survivors: histological characteristics and relationships to radiation and hepatitis B and C viruses. *J Radiat Res* 2001;**42**:117–30.

3. Molinari M, Kachura JR, Dixon E *et al*. Transarterial chemoembolisation for advanced hepatocellular carcinoma: results from a North American cancer centre. Clin Oncol (R Coll Radiol) 2006;**18**:684–92.
4. Ma S, Jiao B, Liu X *et al*. Approach to radiation therapy in hepatocellular carcinoma. *Cancer Treat Rev* 2010; **36**:157–63.
5. Wu SS, Yen HH, Chung CY. Oesophageal variceal bleeding in hepatocellular carcinoma with portal vein thrombosis: improved outcome in response to molecular target therapy. *Clin Oncol (R Coll Radiol)* 2008;**20**:566–7.
6. Seong J, Park HC, Han KH *et al*. Clinical results and prognostic factors in radiotherapy for unresectable hepatocellular carcinoma a retrospective study of 158 patients. *Int J Radiat Oncol Biol Phys* 2003;**55**:329–36.
7. Tse RV, Guha C, Dawson LA *et al*. Conformal radiotherapy for hepatocellular carcinoma. *Crit Rev Oncol Hematol* 2008;**67**:113–23.
8. Merle P, Mornex F, Trepo C *et al*. Innovative therapy for hepatocelluar carcinoma: three-dimensional high-dose photon radiotherapy. *Cancer Lett* 2009;**286**:129–33.
9. Gu K, Lai ST, Ma NY *et al*. Hepatic regeneration after sublethal partial liver irradiation in cirrhotic rats. *J Radiat Res* 2011;**52**:582–91.
10. Sharp GC, Lu HM, Trofimov A *et al*. Assessing residual motion for gated proton-beam radiotherapy. *J Radiat Res* 2007;**48** Suppl:A55–9.
11. Eccles C, Brock KK, Bissonnette JP *et al*. Reproducibility of liver position using active breathing coordinator for liver cancer radiotherapy. *Int J Radiat Oncol Biol Phys* 2006;**64**:751–9.
12. Zhao JD, Xu ZY, Zhu J *et al*. Application of active breathing control in 3-dimensional conformal radiation therapy for hepatocellular carcinoma: the feasibility and benefit. *Radiother Oncol* 2008;**87**:439–44.
13. Wong JW, Sharpe MB, Jaffray DA *et al*. The use of active breathing control (ABC) to reduce margin for breathing motion. *Int J Radiat Oncol Biol Phys* 1999;**44**:911–9.
14. Xi M, Liu MZ, Deng XW *et al*. Defining internal target volume (ITV) for hepatocellular carcinoma using four-dimensional CT. *Radiother Oncol* 2007;**84**:272–8.
15. Dobashi S, Sugane T, Mori S *et al*. Intrafractional respiratory motion for charged particle lung therapy with immobilization assessed by four-dimensional computed tomography. *J Radiat Res* 2011;**52**:96–102.
16. Mori S, Lu HM, Wolfgang JA *et al*. Effects of interfractional anatomical changes on water-equivalent pathlength in charged-particle radiotherapy of lung cancer. *J Radiat Res* 2009; **50**:513–9.
17. Palma DA, Verbakel WF, Otto K *et al*. New developments in arc radiation therapy: A review. *Cancer Treat Rev* 2010; **36**:393–9.
18. Dawson LA, Brock KK, Kazanjian S *et al*. The reproducibility of organ position using active breathing coordinator (ABC) during liver radiotherapy. *Int J Radiat Oncol Biol Phys* 2001;**51**:1410 –21.
19. Xi M, Liu MZ, Zhang L *et al*. How many sets of 4D-CT images are sufficient to determine internal target volume for liver radiotherapy? *Radiother Oncol* 2009;**92**:255–9.
20. Velec M, Moseley JL, Eccles CL *et al*. Effect of breathing motion on radiotherapy dose accumulation in the abdomen using deformable registration. *Int J Radiat Oncol Biol Phys* 2011;**80**:265–72.
21. Méndez Romero A, Zinkstok RT, Wunderink W *et al*. Stereotactic body radiation therapy for liver tumors: impact of daily setup corrections and day-to-day anatomic variations on dose in target and organs at risk. *Int J Radiat Oncol Biol Phys* 2009;**75**:1201–8.
22. Kavanagh BD, Pan CC, Dawson LA *et al*. Radiation dose–volume effects in the stomach and small bowel. *Int J Radiat Oncol Biol Phys* 2010;**76**:101–7.
23. Cilla S, Macchia G, Digesù C *et al*. 3D-conformal versus intensity-modulated postoperative radiotherapy of vaginal vault : A dosimetric comparison. *Med Dosim* 2010;**35**: 135–42.
24. Shaffer R, Nichol AM, Vollans E *et al*. A comparison of volumetric modulated arc therapy and conventional intensity-modulated radiotherapy for frontal and temporal high-grade gliomas. *Int J Radiat Oncol Biol Phys* 2010;**76**:1177–84.
25. Popescu CC, Olivotto IA, Beckham WA *et al*. Volumetric modulated arc therapy improves dosimetry and reduces treatment time compared to conventional intensity-modulated radiotherapy for locoregional radiotherapy of left-sided breast cancer and internal mammary. *Int J Radiat Oncol Biol Phys* 2010;**76**,287–95.
26. Shaffer R, Morris WJ, Moiseenko V *et al*. Volumetric modulated Arc therapy and conventional intensity-modulated radiotherapy for simultaneous maximal intraprostatic boost: a planning comparison study. *Clin Oncol (R Coll Radiol)* 2009;**21**:401–7.
27. Yin Y, Ma C, Gao M *et al*. Dosimetric comparison of rapidarc with fixed gantry intensity-modulated radiotherapy treatment for multiple liver metastases radiotherapy. *Med Dosim* 2011;**36**:448–54.
28. Hughes S, McClelland J, Chandler A *et al*. A comparison of internal target volume definition by limited four-dimensional computed tomography, the addition of patient-specific margins, or the addition of generic margins when planning radical radiotherapy for lymph node-positive non-small cell lung cancer. *Clin Oncol (R Coll Radiol)* 2008;**20**:293–300.
29. Park HC, Seong J, Han KH *et al*. Dose-response relationship in local radiotherapy for hepatocellular carcinoma. *Int J Radiat Oncol Biol Phys* 2002;**54**:150–5.
30. Chung SI, Seong J, Park YN *et al*. Identification of proteins indicating radiation-induced hepatic toxicity in cirrhotic rats. *J Radiat Res* 2010;**51**:643–50.
31. Pan CC, Kavanagh BD, Dawson LA *et al*. Radiation-associated liver injury. *Int J Radiat Oncol Biol Phys* 2010;**76** Suppl:S94–100.
32. Saito T, Sakamoto T, Oya N *et al*. Predictive factors for lung dose reduction by respiratory gating at radiotherapy for lung cancer. *J Radiat Res* 2010;**51**:691–8.
33. Gong G, Yin Y, Xing L *et al*. Comparison of internal target volumes for hepatocellular carcinoma defined using 3DCT with active breathing coordinator and 4DCT. *Technol Cancer Res Treat* 2011;**10**:601–6.